

# STARS

University of Central Florida  
**STARS**

---


Electronic Theses and Dissertations, 2004-2019

---

2012

## A Novel Link Between Akt1 And Twist1 In Ovarian Tumor Cell Motility And Invasiveness

Nirav Shah  
*University of Central Florida*

 Part of the [Biotechnology Commons](#), and the [Molecular Biology Commons](#)  
Find similar works at: <https://stars.library.ucf.edu/etd>  
University of Central Florida Libraries <http://library.ucf.edu>

This Masters Thesis (Open Access) is brought to you for free and open access by STARS. It has been accepted for inclusion in Electronic Theses and Dissertations, 2004-2019 by an authorized administrator of STARS. For more information, please contact [STARS@ucf.edu](mailto:STARS@ucf.edu).

---

### STARS Citation

Shah, Nirav, "A Novel Link Between Akt1 And Twist1 In Ovarian Tumor Cell Motility And Invasiveness" (2012). *Electronic Theses and Dissertations, 2004-2019*. 2297.  
<https://stars.library.ucf.edu/etd/2297>



A NOVEL LINK BETWEEN AKT1 AND TWIST1 IN OVARIAN TUMOR CELL MOTILITY  
AND INVASIVENESS

by

NIRAV RAJU SHAH

Bachelor of Pharmacy, University of Mumbai, India, 2010

A thesis submitted in partial fulfillment of the requirements  
for the degree of Masters in Science  
in the Department of Biotechnology  
in the Burnett School of Biomedical Sciences, College of Medicine  
at the University of Central Florida  
Orlando, Florida

Summer Term  
2012

Major Professor: Deborah A. Altomare

© 2012 Nirav Raju Shah

## **ABSTRACT**

Ovarian cancer results in more deaths per year than any other cancer of the female reproductive system. The low survival rate is partly due to the lack of early detection and the susceptibility to relapse. The AKT serine threonine kinase plays a pivotal role in hallmark cellular processes for the progression of ovarian cancer, including tumor cell growth and migration. Therapeutic targeting of pan-AKT has been problematic, in part due to feedback mechanisms and crosstalk with other pathways. The hypothesis for this study is that AKT 1, -2 and -3 isoforms may have different roles and regulate cell processes in uniquely varied ways. A transgenic mouse model that expresses the SV40 T-antigen viral oncogene and is known to have dramatically increased susceptibility to ovarian cancer was utilized, and it had genetic inactivation of either AKT1 or AKT2 through targeted deletion of the individual genes because these isoforms have been implicated in this cancer. Primary ovarian tumor cell cultures were established and found to exhibit different morphology, proliferation and migration that may indicate a different role for the AKT1 and AKT2 isoforms in these contexts. Ovarian tumor cells with absence of AKT1 predominantly exhibited reduced cell migration when compared to cells with retention of AKT1 and absence of AKT2. Since AKT is known to be important for epithelial-mesenchymal transition (EMT), a process potentially associated with tumor cell metastasis, the expression of transcription factors implicated in EMT was assessed by real-time array analysis in ovarian tumor cells knocked-out for either AKT1 or AKT2. Twist1, one of the major players in EMT, was not detectable in the cells missing the AKT1 isoform. Results indicate an association of Twist1 with AKT1 in EMT and migration of ovarian tumors cells. This finding is significant because AKT2 has been implicated as the major player of cell migration in human breast cancer

cells. Collectively, these findings support a tissue specific role of the AKT isoforms, and may provide insights regarding the most useful cell context in order to target components of the AKT signaling pathway indirectly affecting EMT in order to prevent tumor progression in patients with ovarian and perhaps other types of cancers.

## ACKNOWLEDGMENTS

There are not enough words that suffice to express my gratitude to my mentor, principal investigator and committee chair Dr. Deborah Altomare. Her invaluable insight, patience and immense knowledge about the subject matter have helped me shape up my project with utmost novelty and precision. Her recommendation and moral support has helped me lay a strong foundation for my future ventures. I would also like to acknowledge the time and support of my esteemed committee members Dr. Annette Khaled and Dr. Jihe Zhao. Their guidance was very helpful throughout my project.

I also wish to thank our very dear lab manager Lina Spinel who helped me learn many techniques and supported me immensely with her time and skills throughout my project. Special thanks to my colleagues, Veethika Pandey and Lisette Dominguez for their contribution. All other lab members have always been very supportive and encouraged me to sail through smoothly.

I would like to give a special mention to the various labs at the Lake Nona facility for making it a very productive and collaborative research institute. I wish to thank Dr. Subhrangshu Guhathakurta and other members from Dr. Yoon Seong Kim's lab for their support. Insights from Shahnawaz Jiwani from Dr. Travis Jewett's lab, Rebecca Boohaker and other members from Dr. Khaled's lab proved to be very helpful. Thanks to Dr. Masternak's lab for their support.

Special thanks to my second family away from home, my friends, Mona Doshi and Himansu Shekhar Pattanaik, Taranjeet Singh Bhatia, Rakshath Kashyap, Parth Patel for their moral support.

Last but not the least my perennial gratitude to my parents, only second to GOD almighty, for giving me the strength and encouragement to achieve my dream and ultimate goal of becoming a responsible human being offering my dedication for the betterment of humanity.

## TABLE OF CONTENTS

CHAPTER 1. INTRODUCTION .....	1
1.1 Ovarian Carcinoma .....	1
1.2 PI3K/AKT signaling pathway.....	2
1.3 Isoforms of AKT.....	3
1.4 Epithelial Mesenchymal Transition (EMT) .....	5
1.5 Molecular regulation of EMT in general .....	7
1.6 EMT in ovarian cancer.....	9
CHAPTER 2. MATERIALS AND METHODS .....	11
2.1 Cell Culture and Experimental Conditions .....	11
2.2 Reagents and Antibodies.....	11
2.3 Cell Migration/ Wound Healing Assay.....	12
2.4 Cell Invasion/ Matrigel Assay .....	12
2.5 Induction of Epithelial Mesenchymal Transition .....	13
2.6 RNA Isolation .....	13
2.7 Real Time PCR/ Array Analysis.....	14
2.8 Protein Extraction .....	17
2.9 Western Blot Analysis .....	18
CHAPTER 3. RESULTS .....	20
3.1 Western Blots showing isoform knockouts at protein level .....	20
3.2 Cell Migration/ Wound Healing Assay.....	21
3.3 Cell Invasion/ Matrigel Assay .....	23



3.4 Induction of EMT .....	25
3.5 RT <sup>2</sup> Profiling using EMT array (PAMM-090 SAbiosciences).....	27
3.6 Validation at Protein levels.....	38
CHAPTER 4. DISCUSSION.....	39
REFERENCES .....	44

## LIST OF FIGURES

Figure 1 Activation of PI3K/Akt signaling pathway. ....	2
Figure 2 General scheme of major molecules in EMT .....	7
Figure 3 General schematic showing inhibition of E-cadherin expression and increase in N-cadherin expression by the transcriptional regulators Twist, Snail and Slug. ....	8
Figure 4 Procedure of Profiling RNA .....	17
Figure 5 Western blot confirming AKT isoform specific knockout cells .....	20
Figure 6 Cell Migration Assay showing images of the three representative cell types 0174 Akt1 nulls, 0148 Akt2 nulls, and 01235 control tumor cells taken at regular intervals till 24 hours. ....	21
Figure 7 DAPI stained nuclei in representative fields of the three cell types .....	23
Figure 8 Quantitative comparison of the invaded cells between three cell types .....	24
Figure 9 Change in morphology from epithelial to mesenchymal at 48 hours and 72 hours using TGF $\beta$ 1 and EGF synergy. These images are representative of experiment performed in triplicates. ....	25
Figure 10 Comparison of fold change regulation of Twist1 expression levels in 01235 tumor cells with retention of Akt1 and Akt2 (controls), 0174 Akt1nulls and 0148 Akt2 nulls .....	32
Figure 11 Comparison of fold change regulation of Snai2 (Slug) expression levels in 01235 tumor cells with retention of Akt1 and Akt2 (controls), 0174 Akt1nulls and 0148 Akt2 nulls ...	33
Figure 12 Comparison of fold change regulation of Snai2 (Slug) and Twist1 expression levels in 01235 tumor cells with retention of Akt1 and Akt2 (controls), 0174 Akt1nulls and 0148 Akt2 nulls with and without induction of EMT .....	34
Figure 13 Validation of real time findings using protein band determination. ....	38
Figure 14 A Schematic, indicating the series of events that may explain the observations in the cell model. ....	41

## LIST OF TABLES

Table 1 Genomic DNA elimination mix preparation .....	15
Table 2 Reverse Transcription Mix .....	15
Table 3 PCR components mix .....	16
Table 4 Cell counts before Cell migration Assay .....	22
Table 5 Cell count before Matrigel Assay .....	23
Table 6 Concentration and Purity of Isolated RNA from samples with and without induction of EMT for RT <sup>2</sup> profiling .....	27
Table 7 GENE Table listing the genes probed in RT <sup>2</sup> PCR Array Profiling .....	29
Table 8 P-values of Snai2 and Twist1 calculated from the samples in triplicates of the groups with and without EMT induced. ....	35
Table 9 Fold regulation values determining over or under expression of genes in 0174 Akt1 null cells when compared to 01235 controls. ....	35
Table 10 Fold regulation values determining over or under expression of genes in 0148 Akt2 null cells when compared to 01235 controls. ....	36
Table 11 Fold regulation values determining over or under expression of genes in 0174 Akt1 null cells when compared to 0148 Akt2 null. ....	37

# CHAPTER 1. INTRODUCTION

## 1.1 Ovarian Carcinoma

Ovarian cancer is the fifth most common type of cancer causing fatalities in women. This second-most deadly gynecological disorder was diagnosed in 21,880 women in United States, causing 13,850 estimated deaths in the year 2010 (Jemal, Siegel et al. 2010). Treatment options include surgery and administration of carboplatin and paclitaxel as combination chemotherapy. Intensive chemotherapy has improved the 5- year survival rate by 8% in the past 30 years. However most patients are presented at an advanced FIGO stage III-IV which increases the mortality rate along with acquired resistance to chemotherapy (Agarwal and Kaye 2003) (Cannistra 2004) (Hennessy, Coleman et al. 2009) (Davidson, Trope et al. 2012). This shows the aggressive nature of ovarian carcinoma. Only 20% of the patients diagnosed with ovarian cancer are in their first stage and can be completely cured by intensive treatments. Ninety percent of the ovarian malignancies are initiated by the cancer cells arising from the epithelial cells of the surface of ovary (Shan and Liu 2009). The outer surface of the ovary is surrounded by a single layer of peritoneal mesothelium, which is termed as ovarian epithelium. It is said to be a derivative of celomic epithelial cells, which is responsible for generation of female reproductive organs (Connolly, Bao et al. 2003). It is thought that the pluripotent potential of ovarian cancer cells to differentiate into various cancer cell types is due to their celomic epithelial cell origin (Connolly, Bao et al. 2003). According to the differentiation of the tumor cells, ovarian cancer is

divided into four major types- serous, endometriod, mucinous and clear cell. Serous is the most common type of ovarian cancer and is further categorized into low grade and high grade serous tumors (Landen, Birrer et al. 2008) (Cho and Shih Ie 2009). It is postulated that mutations in KRAS/BRAF genes, (Singer, Oldt et al. 2003) unbalanced regulation of p53 & BRCA1/2 and Wnt/ $\beta$ -catenin/TCF pathways, mutation in the PTEN tumor suppressor and activation of phosphoinositide 3-kinase (PI3 kinase)/AKT pathway, form the genetic basis of epithelial ovarian cancer (Yap, Garrett et al. 2008). The main focus of my project is the AKT pathway and the role of the two isoforms of AKT (AKT1 and AKT2) in epithelial ovarian cancer cells.

### 1.2 PI3K/AKT signaling pathway

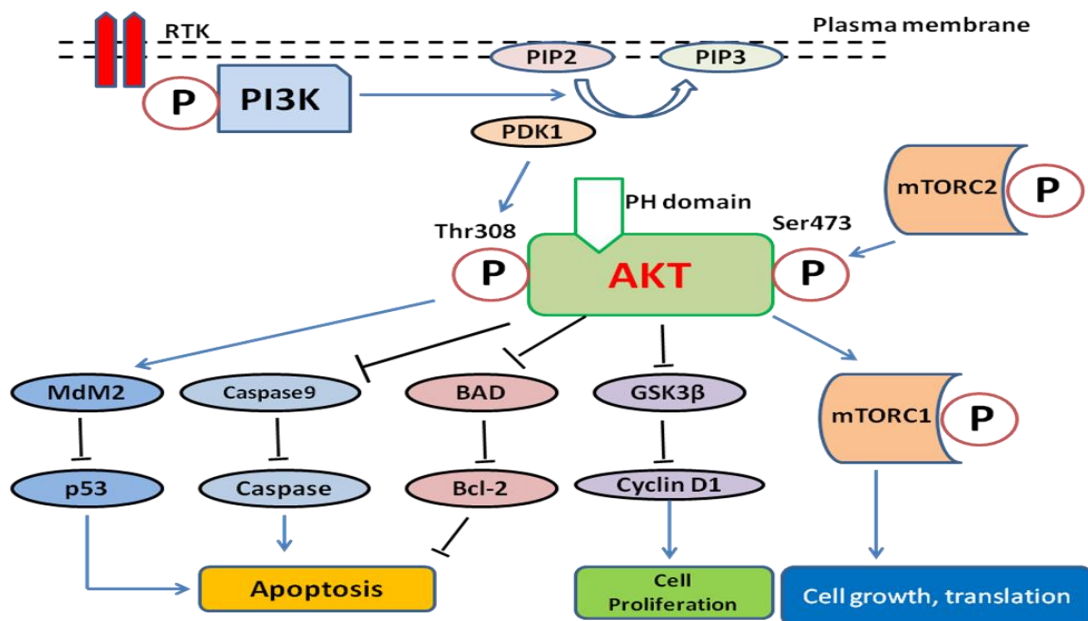


Figure 1 Activation of PI3K/Akt signaling pathway.

The serine/threonine kinase AKT/protein kinase B, which serves as a downstream target of PI3 kinase, has key roles in the regulation of cell growth and proliferation, survival, motility and metabolism (Bellacosa, Testa et al. 1991). G protein coupled receptors and tyrosine kinases activate PI3 kinase by phosphorylation. This in turn generates phosphoinositides. AKT translocates from the cytosol to the plasma membrane where the pleckstrin homology (PH) domain binds phosphatidylinositol (3, 4, 5)-trisphosphate (PIP3). AKT is phosphorylated in the C-terminal regulatory domain (RD) on Thr308 by PDK1 and Ser473 by mTORC2 (Vivanco and Sawyers 2002). This activated AKT performs a plethora of necessary cellular functions such as prevention of apoptosis by enhancing glucose utilization, increasing the levels of Bcl-2 or Bcl-x1; (Maestro, Dei Tos et al. 1999) enhancing nuclear localization of MDM2, (Mayo and Donner 2001) activation of NF- $\kappa$ B pathway, inhibition of cytochrome C release from mitochondria, inactivation of Bad and Bax (Testa and Bellacosa 2001). Akt contributes to cancer progression by inhibiting p21, p27, GSK3 $\beta$  and activating mTOR (Nicholson and Anderson 2002).

### **1.3 Isoforms of AKT**

AKT is found as three isoforms AKT-1, -2, and -3. All three exhibit high sequence homology. The genes reside on different human chromosomes. Due to less sequence homology between the C- and N- terminal domains of the three isoforms it is believed that they have different physiological and biological functions in normal as well as cancer cells (Cheng, Ruggeri et al. 1996). It has been observed that AKT1 is uniformly expressed in various organs. Over expression of wild type AKT2 has been shown to transform the NIH 3T3 cells (Bellacosa,

de Feo et al. 1995). Overexpression of AKT2 is seen in 15% of ovarian cancer and 20% of pancreatic cancer (Carpten, Faber et al. 2007). Recently it has been studied that mutation in the PH domain of AKT1 promotes its localization to the plasma membrane and it has been studied to transform cells in vitro and induce leukemia in mice (Altomare and Testa 2005). Over activation of AKT kinase due to mutation in itself or upstream signaling molecules is found in 50% of human tumors making it a highly attractive target for anti-cancer therapy (Irie, Pearlman et al. 2005). Recently there has been speculation for opposing roles for the AKT1 and AKT2 isoforms in cell motility and invasion. In human breast cancer cell lines AKT1 has shown to be an inhibitor of cell motility. Knockdown studies showed that a decrease in the levels of AKT1 increased cell motility whereas a decrease in AKT2 did not show substantial effect. Down-regulation of AKT1 caused an increase in ERK, which was supposed to give anti-migratory property to AKT1 (Yoeli-Lerner, Yiu et al. 2005). A conflicting study carried out in breast cancer cell lines published that an anti-migratory effect of AKT1 was independent of the ERK pathway. AKT1 mediated activation of MDM2 ubiquitin ligase resulted in proteosomal degradation of NFAT- nuclear factor of activated T cells, which is a pro-migratory transcription factor (Liu, Radisky et al. 2006). Another study in mammary epithelial breast cancer cells expressing myristoylated (myr) AKT1 corroborated the anti-migratory role of AKT1, but proposed a completely different mechanism. Phosphorylation of targeted tumor suppressor tuberous sclerosis complex 2 (TSC2) and its degradation was found in cells over expressing myr-AKT1. This led to a reduction in Rho-GTPase levels and a decrease in focal adhesions and actin stress fibers to reduce cell motility and invasion (Liu, Radisky et al. 2006). A recent publication linked Twist, a transcription factor implicated in epithelial mesenchymal transition with AKT2 to

cause its up-regulation and induce cell motility and invasion (Cheng, Chan et al. 2007) . All these studies, which were carried out in breast cancer cell lines, established the conflicting roles of AKT1 and AKT2 in cell migration and invasion. Recent studies in non-small cell lung cancer showed that AKT1 is predominant regulator of cell proliferation and migration whereas AKT2 is largely inconsequential (Lee, Kim et al. 2011). Thus the different roles of AKT1 and AKT2 become a matter of cell context and it could be possible to find totally reversed roles of the two isoforms in a different organ/cell type. In our lab we are equipped with a transgenic mouse model that expresses the SV40 T antigen viral oncogenes in ovarian cells; the mice were genetically inactivated either for AKT1 or AKT2 and are predisposed to forming ovarian tumors and derived at least two different cell lines with targeted deletion of the individual genes. This unique model has helped me to delineate the distinct roles of AKT1 and AKT2 in ovarian cancer cells. The transcription factors that regulate both the isoforms can be highlighted and their role in epithelial mesenchymal transition can be defined.

#### **1.4 Epithelial Mesenchymal Transition (EMT)**

A very complex and interesting phenomenon in which, epithelial cells that line the organs and tissues, are transitioned into becoming spindle shaped mesenchymal cells and gain motility, is called Epithelial Mesenchymal Transition (EMT) (Yang and Weinberg 2008). EMT is desirable and quite important during embryogenesis, tissue fibrosis and wound healing, it occurs in a controlled fashion and is brought about by various events of molecular transformations in a cell which triggers the phenotypic switch in the cell to become stem like from the current



epithelial phenotype (Yang and Weinberg 2008). As mentioned earlier there is a constant inter-conversion between the two phenotypes, epithelial and mesenchymal during embryogenesis. This inter-conversion is necessary for the formation of different germ layers and helps the differentiated cells reach their destination. Once the cells gain motility and reach their destination there is an event of reverse EMT called MET mesenchymal to epithelial transition, which helps them revert to an epithelial phenotype. Similar pattern has been observed in highly metastatic cancer. (Thompson, Newgreen et al. 2005).

In order to understand the logic behind this conversion of cells from one phenotype to other it is important to learn the distinct features of the two phenotypes. Epithelial cells possess adherent interactions, which are cohesive in nature and form epithelial sheets of the cells that line the organ or tissue. These sheets are held together by tight junctions and desmosomes, which are in turn supported by surfactant molecules like E-cadherin, ZO-1, keratins and collagen. The epithelial cells demonstrate a very nice tissue framework, the cells are rested on a basal surface at one end and the upper layer is free. The epithelial cells are thus termed to be bipolar in nature. (Thompson, Newgreen et al. 2005).

Mesenchymal cells lack the cellular framework as seen in the epithelial cells. They have reduced adhesive property but can still stay together while moving towards their destination. They do not have a basement membrane as in the case of epithelial tissue network. The major molecules that impart mesenchymal properties to these cells are N-cadherin, fibronectin, Vimentin and some others. Various transcription factors are implicated in this process of transition from epithelial to mesenchymal phenotype.(Thompson, Newgreen et al. 2005).

Summarizing the basics of EMT, it is clear that in this phenomenon the cells lose their epithelial characteristics like strong tissue framework and become more flexible and motile in phenotype which is very close to being a stem cell. There is a plethora of molecular events that facilitate this process and its reverse as well. Intensive research is being done in this area especially after the implication of EMT in cancer metastasis. (Thiery, Acloque et al. 2009).

### 1.5 Molecular regulation of EMT in general

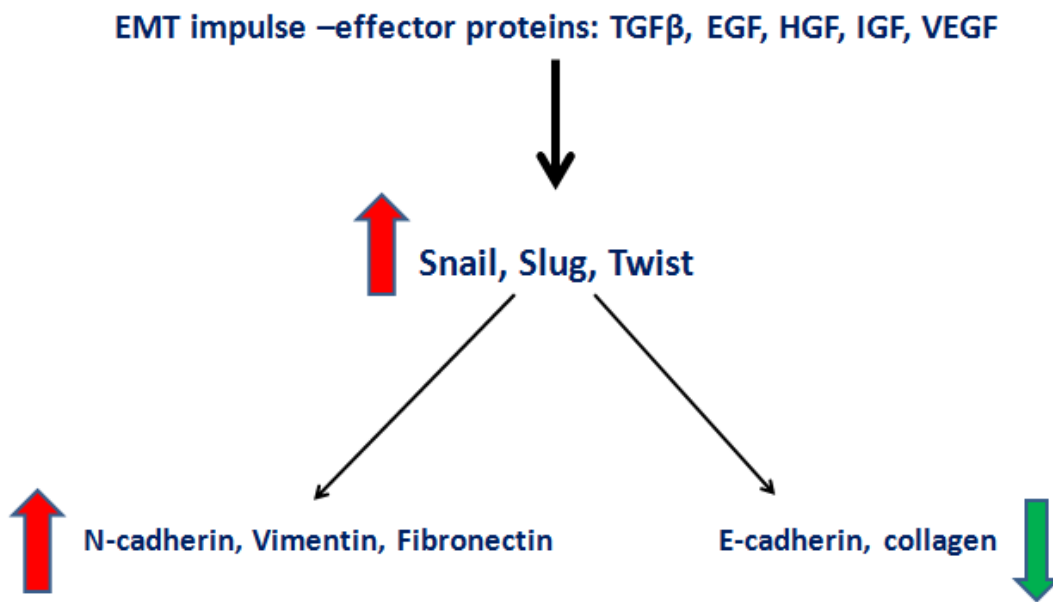


Figure 2 General scheme of major molecules in EMT

Various growth factors play a vital role in inducing EMT during embryogenesis as well as cancer progression. Among the wide variety of growth factors the main players are transforming growth factor beta 1 (TGF  $\beta$ 1), epidermal growth factor (EGF), fibroblast growth factor (FGF), platelet-derived growth factor (PDGF), insulin like growth factor (IGF), vascular

endothelial growth factor (VEGF), Prostaglandin E2, stem cell growth factor, parathyroid hormone, bone morphogenetic proteins (BMP) and hepatocyte growth factor (HGF) (Kalluri and Weinberg 2009). Along with the morphological changes there are a number of events causing either up regulation or down regulation of various molecules, which can, in general, be identified as molecular markers of EMT. The markers that are generally down regulated include E-cadherin, Claudins, ZO-1, cytokeratins, occludin, MUC1, laminin- 1, entactin and microRNA 200 family. The over expressed markers comprise of molecules namely, transcription factors like Twist, Snail, Slug, Zeb1, SIP1, KLF8, Goosecoid, FoxC2 as well as Vimentin, fibronectin and miR10b. (Zeisberg and Neilson 2009) (Thiery, Acloque et al. 2009) (Davidson, Trope et al. 2012). Most of the molecules mentioned above are altered during the process of embryonic development as well as metastasis. The only difference between the two processes is that in the later, the cells lose their target recognition specificity and there is activation of autocrine loops as well as enhanced angiogenesis, all of which support aggressive tumor growth and metastasis (Ahmed, Thompson et al. 2007).

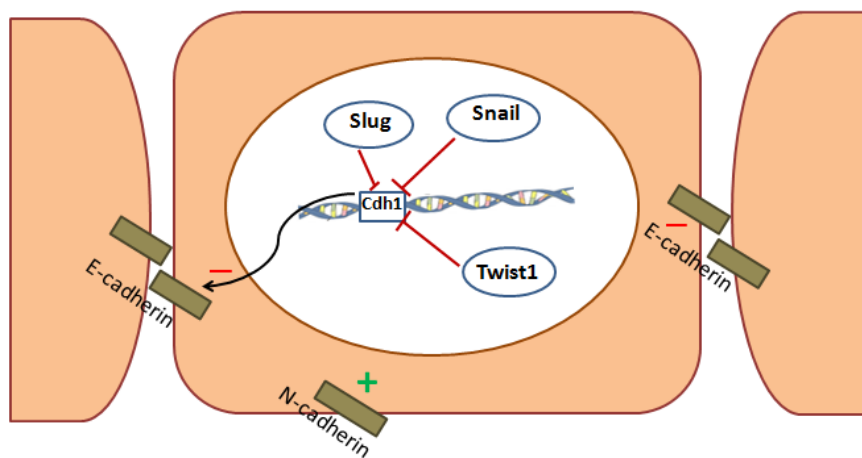


Figure 3 General schematic showing inhibition of E-cadherin expression and increase in N-cadherin expression by the transcriptional regulators Twist, Snail and Slug.

## **1.6 EMT in ovarian cancer**

This complex phenomenon is being studied in depth and with every significant observation it is being repeatedly proved that EMT in ovary is an exception to the norm (Sundfeldt, Ivarsson et al. 2001). One of the most common markers of EMT in majority of the tissues undergoing metastasis is decrease in E-Cadherin expression and increase in its N-Cadherin counterpart. Although increased levels of soluble E-Cadherin have been reported in cyst fluids of malignant ovarian tumors (Davidson 2001), there are reports of either the E-Cadherin expression levels being increased or them remaining the same as in normal ovarian tissue (Christiansen and Rajasekaran 2006). This non-canonical observation was also rationalized by stating that the up regulation of E-cadherin indicated the survival signals for the cancer cell or transition to mesenchymal to epithelial phenotype after EMT (Patel, Madan et al. 2003). Ovarian tumor masses that progress to advanced tumor stages have also been reported to have enhanced expression P-Cadherin (Alipio, Jones et al. 2011).

The cadherin levels are highly regulated by hallmark players of EMT reported as Snail, Slug, Zeb family, Twist family and several other factors. The regulation of these players is poorly understood *in vitro* as well as at the clinical tier. It can be stated with the present literature that expression profiles of EMT related molecules are significantly different in ovarian cancer cells when compared to other types of cancer. This includes higher levels of E-Cadherin and SIP1 and reduced expression of Snail, Slug, Twist and Zeb family.

These nuances make ovarian carcinoma progression unique in its own way and raise a lot of unanswered questions. Although the studies are not able to completely define EMT in ovarian cancer, there is compelling evidence which links EMT to various signaling mechanisms present in the cell. The cross talk between the signaling pathways in the presence and absence of EMT, and also sometimes contributing to EMT, is very interesting and an in-depth study of this area could uncover certain hidden facts, which might prove to be important therapeutic targets in the treatment of ovarian carcinoma.

In this project there have been developments which link Akt isoform specificity to some major players in EMT.

## **CHAPTER 2. MATERIALS AND METHODS**

### **2.1 Cell Culture and Experimental Conditions**

Ovarian surface epithelial tumor cells were cultured in Dulbecco's Modification of Eagle's Medium (DMEM) supplemented with 10% fetal bovine serum, L-glutamine and penicillin-streptomycin. Experiments were performed with cells in passage 12-20. Confluent cells were dissociated using 0.05% Trypsin. The cells were maintained in 37°C, 5 % CO<sub>2</sub> incubator under sterile conditions.

### **2.2 Reagents and Antibodies**

Murine TGF  $\beta$ 1 (#5231LF; lot 3) was purchased from Cell Signaling Technology, Inc. Antibodies against Akt1 (#2938S; lot 2), Akt2 (#3063; lot 4), total Akt (#9272; lot 17),  $\beta$ -actin (#MAB1501; lot NG1848416), N-cadherin (#2019-1; lot YE011803R) and E-cadherin (#3195; lot 10) were also purchased from Cell Signaling Technology, Inc. Murine Epidermal growth factor EGF (#53003-018) was purchased from Invitrogen.

### **2.3 Cell Migration/ Wound Healing Assay**

A 24-well plate format cell migration assay kit (Cell Biolabs, Inc.) was used. In brief, the wells had a gel spot in the center, which was biocompatible but did not allow cells to adhere to it. The wells to be used were pretreated by adding 500  $\mu$ l of gel pretreatment solution (Cell Biolabs, Inc.) and incubating the plate at room temperature for 20 minutes. The wells were then treated with gel wash solution and incubated at room temperature for 60 minutes. AKT1 nulls, AKT2 nulls and control tumor cells were seeded in three different pretreated wells at the density of  $5 \times 10^5$  cells per well in 500  $\mu$ l of media. The cells were allowed to attach for 5 hours. The wells were treated with the gel removal agent for 30 minutes at 37°C. Gel removal agent was prepared by diluting 100 X gel removal agent (Cell Biolabs, Inc.) to 1X in media. The wells were repeatedly washed three times with media and 1 ml of fresh media was administered. The wells were photographed every 2 hours starting at 0 hour being the time the gel spot was removed using the gel removal agent.

### **2.4 Cell Invasion/ Matrigel Assay**

BD BioCoat Matrigel Invasion chambers were used to gauge invasive potential of the cells. 500  $\mu$ l warm media was added to the determined inserts and the companion wells to rehydrate them. The media was carefully removed after 2 hours and fresh media was added to the companion wells. The cells were prepared by suspending them in DMEM. The cells were counted using a TC10 automated cell counter (Bio-Rad Laboratories) and diluted to  $5 \times 10^4$  cells

per ml. The cells were added on the top layer of the membrane in the inserts. The invasion chambers were incubated at 37°C, 5% CO<sub>2</sub> for 22 hours. The non-invaded cells were swabbed off the upper surface of the Matrigel-coated membrane using sterile cotton swabs by applying gentle but firm pressure. The scrubbing was repeated using swabs moistened in media. The invaded cells were fixed using 4% paraformaldehyde for 10 minutes. The fixed cells were stained using a nuclei staining dye, 4', 6-diamidino-2-phenylindole (DAPI) for 2 minutes. The inserts with the fixed stained cells were mounted on a slide with a drop of oil.

### **2.5 Induction of Epithelial Mesenchymal Transition**

Cells were seeded in 6-well plates at the density of 10<sup>5</sup> per ml and nourished with culture media containing 10% FBS. After 24 hours media with 5% FBS was introduced in the cells along with 2 µl of 100 µg/ml TGF β1 and 10 µl of 100 ng/ml of EGF. The effect on the morphology of the cells was observed microscopically every 24 hours.

### **2.6 RNA Isolation**

RNA was isolated using TRIzol reagent (Ambion). 1 ml of TRIzol reagent was added to each well in the 6 well plates. The cells were scrapped off using a cell scraper and collected in sterile 1.5 ml tubes. The tubes were incubated for 5 minutes at room temperature for complete homogenization and dissociation of the nucleoprotein complex. 200 µl of chloroform was added to the tubes. The tubes were capped securely and vortexed for 15 seconds. They were allowed to



incubate at room temperature for 3 minutes. The samples were centrifuged at 12,000 x g for 15 minutes at 4°C. The aqueous phase was removed carefully and transferred into a new tube. 500 µl of 100% isopropanol was added to the aqueous phase. The tubes were incubated at room temperature for 10 minutes. They were centrifuged at 12,000 x g for 10 minutes at 4°C. The supernatant was then removed and 1 ml of 75% ethanol was added to the RNA pellet. The sample was vortexed briefly and centrifuged at 7,500 x g for 5 minutes at 4°C. The RNA was air dried for 10 minutes and resuspended in 50 µl of RNase free water. RNA solution was incubated at 65°C for 5 minutes and then cooled on ice for 2 minutes.

### **2.7 Real Time PCR/ Array Analysis**

RT<sup>2</sup> Profiler PCR Arrays are provided in 96-well plate format. (SAbiosciences, Qiagen). These plates contain 84 primer assays for EMT and 5 housekeeping genes. In addition, one well contains genomic DNA control, 3 wells contain reverse transcription controls and 3 wells contain positive PCR control.

Fresh RNA was isolated as mentioned in the section 2.6 of Material and Methods. After extraction, the RNA, it was dissolved in 50 µl of RNase free water. The tubes containing RNA were briefly left open and heated at 65°C for 5 minutes in a water bath. The tubes were then cooled on ice for 2 minutes. The RNA concentration was determined using a Nanodrop machine (Thermo Scientific). Concentration and purity of RNA were calculated.

In order to prepare cDNA using the RT<sup>2</sup> First Strand Kit provided by Qiagen, RNA concentration was determined and was scaled to use exactly 2 µg of total RNA.

Table 1 Genomic DNA elimination mix preparation

<b>Component</b>	<b>Amount per reaction</b>
RNA	Scaled to 2 µg total RNA
Buffer GE DNA elimination mix	2 µl
RNase free water	Volume adjusted to 10 µl
<b>Total Volume</b>	<b>10 µl</b>

The reagents of the RT<sup>2</sup> First Strand Kit were thawed and briefly centrifuged to bring the contents to the bottom of the tubes. The genomic DNA elimination mix was prepared according to Table 1. The mix was incubated for 5 minutes at 42°C, and then placed immediately on ice for at least 1 minute.

Table 2 Reverse Transcription Mix

<b>Component</b>	<b>Volume per reaction</b>
5x Buffer BC3	4 µl
Control P2	1 µl
RE2 reverse transcriptase mix	2 µl
RNase free water	3 µl
<b>Total Volume</b>	<b>10 µl</b>

The reverse-transcription mix was prepared according to Table 2. 10 µl of reverse-transcription mix was added to each tube containing 10 µl of genomic DNA elimination mix. It was mixed gently by pipetting up and down.

This 20  $\mu\text{l}$  mix was incubated at 42°C for exactly 15 minutes. The reaction was immediately stopped by incubating it in 95°C for 5 minutes. These cycles were carried out in a thermo cycler (Eppendorf Mastercycler).

After the incubation period was over, 91  $\mu\text{l}$  of RNase free water was added to each cDNA synthesis reaction. The contents were mixed gently by pipetting up and down. The reactions were stored in -20°C until they were used for real time experiments. Generally the process of extracting RNA to real time profiling was completed within 48 hours for each sample.

For setting up the real time PCR profiling 96-well plate RT<sup>2</sup> SYBR Green Mastermix was used provided by Qiagen. The tube was briefly centrifuged to bring the contents to the bottom.

Table 3 PCR components mix

<b>Array format</b>	<b>96- well plate</b>
2x RT <sup>2</sup> SYBR Green Mastermix	1350 $\mu\text{l}$
cDNA synthesis reaction	102 $\mu\text{l}$
RNase free water	1248 $\mu\text{l}$
<b>Total Volume</b>	<b>2700 <math>\mu\text{l}</math></b>

The PCR component mix was prepared in a loading reservoir according to Table 3. 25  $\mu\text{l}$  of this reaction mix was dispensed in each well of the 96-well EMT-PCR plate array. The array was tightly sealed with optical adhesive film. It was centrifuged for 1 minute at 1000 x g at room temperature.

The Applied Biosystems 7500 fast real-time thermo cycler was used and was programmed for 1 cycle for 10 minutes at 95°C followed by 40 cycles each for 15 seconds at 95°C and 1 minute at 60°C. After the run, Ct values were obtained and presented as raw data,

which could be further processed using the PCR data analysis software provided by SABiosciences.

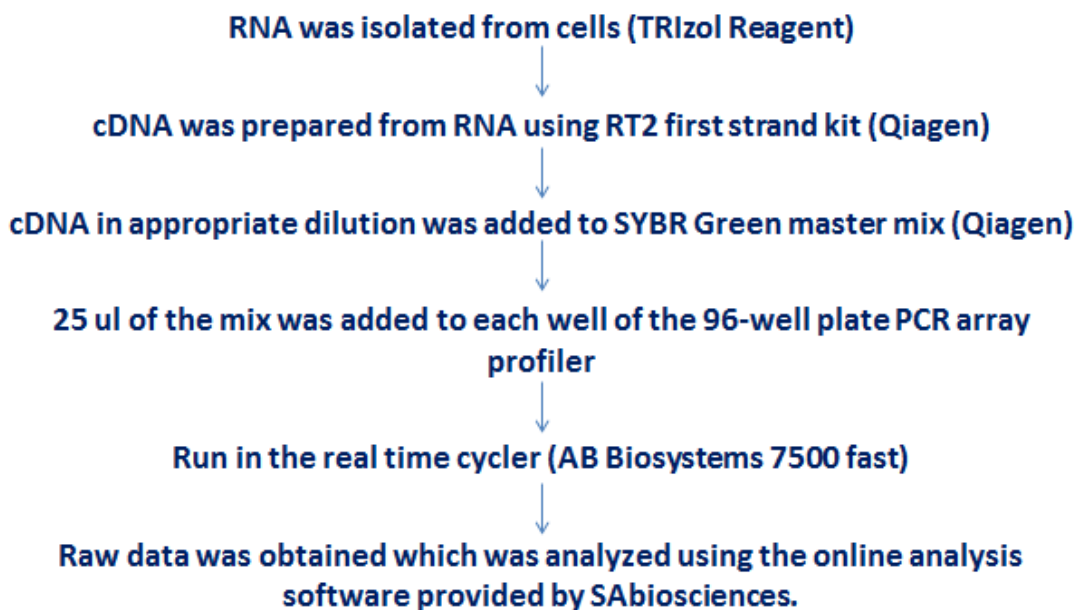


Figure 4 Procedure of Profiling RNA

## **2.8 Protein Extraction**

The media was aspirated from the well containing cells from which protein were to be extracted. Ice-cold PBS was added to the wells. The cells were scrapped off and then suspended in PBS gently using a pipette. The cell suspension was centrifuged in 4°C at 1,100 rpm for 5 minutes. The PBS was pipetted off and depending upon the size of the cell pellet obtained 100-200 µl of ice-cold cell lysis buffer was added to the tubes. The cells were suspended using a pipette. 1 µl of PMSF and 2 ul of proteinase inhibitor cocktail were also added. The tubes were

incubated at  $-80^{\circ}\text{C}$  for 30 minutes. The contents were thawed at room temperature. The contents were centrifuged at 15,000 rpm for 1 min in  $4^{\circ}\text{C}$ . The supernatant was carefully transferred to a new tube which was kept on ice. The supernatant contained the protein and was always kept on ice.

## **2.9 Western Blot Analysis**

12% any-KD SDS-polyacrylamide gels (Bio-Rad) were used for electrophoresis of  $60\ \mu\text{g}$  protein samples. Protein samples were combined with Laemmli's SDS-sample buffer (final 1X) in boiling water for five minutes. Simultaneously, running buffer (10X Tris-SDS-Glycine Running Buffer, pH 8.3, 30.3 g Tris base, 144.0 g glycine and 10 g SDS) was kept in the  $-20^{\circ}\text{C}$  freezer to allow chilling before running electrophoresis. The samples were allowed to cool and were loaded left to right starting with molecular marker. Electrophoresis was run for 15 minutes at 20mA and for 1 hour at 40mA. The gel after electrophoresis was prepared for transfer of protein to a nitrocellulose membrane (GE Healthcare Amersham Hybond ECL Nitrocellulose Membrane). Transfer was done at 25V at  $4^{\circ}\text{C}$  for 2 hours (Invitrogen). Post-transfer the membranes were blocked in blocking agent (5% milk + TBS-Tween (10 ml)), shaking at  $4^{\circ}\text{C}$  overnight or at room temperature for 2 hours. After blocking, the membranes were rinsed twice in TBS-T and then washed 3 times for 5 minutes.

The primary antibody was diluted to optimal concentration in wash buffer or blocking solution (TBS-Tween + milk). The blocked membrane was incubated with diluted primary antibody for 2 hours at room temperature with rocking. The membrane was covered with plastic

to avoid evaporation. The membrane was rinsed two times in TBS, and then washed 3 times for 5 minutes in TBS-Tween (0.1%) rocking at room temperature. The secondary antibodies were diluted to optimal concentration in TBS-Tween + milk. The membrane was rinsed three times in wash buffer (TBS-Tween + milk), followed by 4 times for 5 minutes in wash buffer, shaking at room temperature.

Using advanced chemiluminescent agent (SuperSignal West Dura Stable Peroxide Buffer 1 ml + SuperSignal West Dura Luminol/ Enhancer Solution 1 ml – Thermo Scientific). The membranes were first exposed to this solution, dried and then exposed to an X-ray film (Classic Blue Autoradiography Film BX). The film was developed (AFP image film processor) and thus protein bands were identified.

## CHAPTER 3. RESULTS

### 3.1 Western Blots showing isoform knockouts at protein level

All the available cell types extracted from the transgenic mice were validated at protein levels and it was established that the following cell types were successfully extracted and established under the preferred cell culture conditions:

1. Tumor cells derived from mouse 0174 with Akt1 knockout.
2. Tumor cells derived from mouse 0148 with Akt2 knockout.
3. Tumor cells derived from mouse 0192 with Akt2 knockout.
4. Tumor cells derived from mouse 0109 with retention of Akt1 and Akt2
5. Tumor cells derived from mouse 07D with retention of Akt1 and Akt2.
6. Tumor cells derived from mouse 01235 with retention of Akt1 and Akt2.

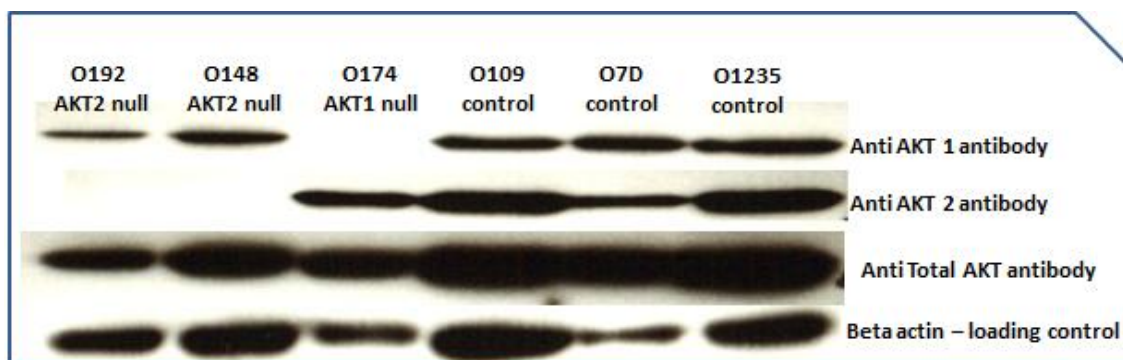


Figure 5 Western blot confirming AKT isoform specific knockout cells

### 3.2 Cell Migration/ Wound Healing Assay

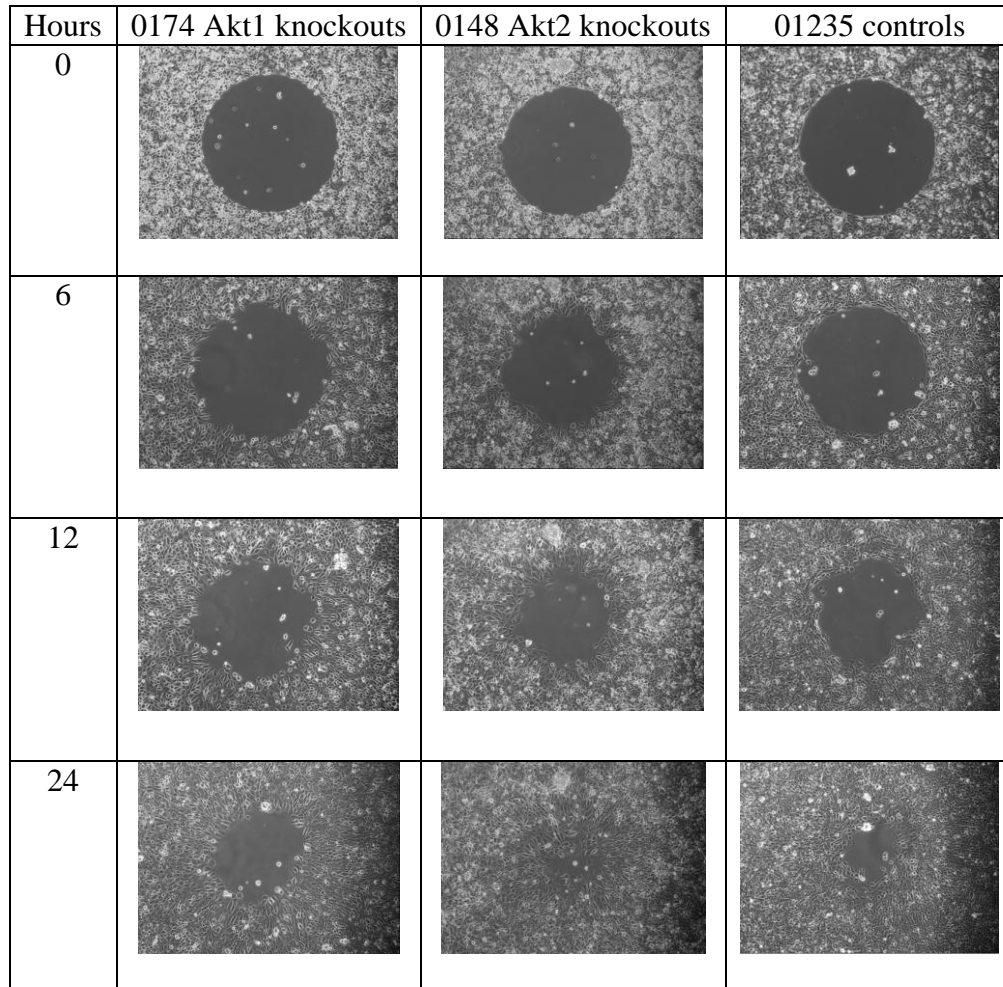


Figure 6 Cell Migration Assay showing images of the three representative cell types 0174 Akt1 nulls, 0148 Akt2 nulls, and 01235 control tumor cells taken at regular intervals till 24 hours.



The experiment was repeated three times. The images of the cells seeded in the cell migration assay 24 well plates, taken at regular time intervals clearly suggest a significant difference among the three cell lines in the time each takes to migrate and occupy the void space.

The three cell types were obtained from ongoing cell culture conditions. After processing the cells for counting, the following counts were obtained. (Images were taken using Zeiss Axio Observer.A1 microscope, AxioCamCc3 camera, EC PCanNeofluar 10x/0.30 Ph1 objective)

Table 4 Cell counts before Cell migration Assay

0174 Akt1 nulls	$2.7 \times 10^6$ cells per ml of media
0148 Akt2 nulls	$2.7 \times 10^6$ cells per ml of media
01235 control tumor cells	$2.8 \times 10^6$ cells per ml of media

The cells were diluted in media to a uniform concentration of  $5 \times 10^5$  cells per 500  $\mu$ l of media.

After seeding  $5 \times 10^5$  cells in each well, the void circular space in the center of the well protected by gel was released of the gel in 4 hours. Upon release of the gel block the cells attached were arranged as shown in the Figure 8 in the 0 hours panel. The experiment was conducted within 28 hours of seeding of cells. This time frame reduced the possibility of cells dividing and occupying the space rather than migration, as the doubling time of the employed cell types was characterized by CFSE cell proliferation staining (Invitrogen) as being more than 24 hours. It was observed that 0148 Akt2 nulls (with retention of Akt1) migrated at a faster rate than 0174 Akt1 nulls. 01235 cells with retention of Akt1 and Akt2 isoforms were not significantly different from 0148 cells in their migration rate. This suggests that Akt1 is important for the cell migration. Loss of Akt1 reduces the cell migration rate to a noteworthy extent.

### 3.3 Cell Invasion/ Matrigel Assay

Table 5 Cell count before Matrigel Assay

0174 Akt1 nulls	$5.6 \times 10^6$ cells per ml of media
0148 Akt2 nulls	$4.4 \times 10^6$ cells per ml of media
01235 control tumor cells	$3.8 \times 10^6$ cells per ml of media

All the three types of cells were prepared in dilutions such that they contained  $5 \times 10^4$  cells per ml of DMEM. 500  $\mu$ l of this cell suspension was added to the upper surface of the membrane and the experiment was performed as mentioned in section 2.4. The DAPI stained lower membrane was observed under the microscope and counts from 10 random fields per cell type were taken. An average of these counts was taken and compared for quantitative analysis of cell invasion.

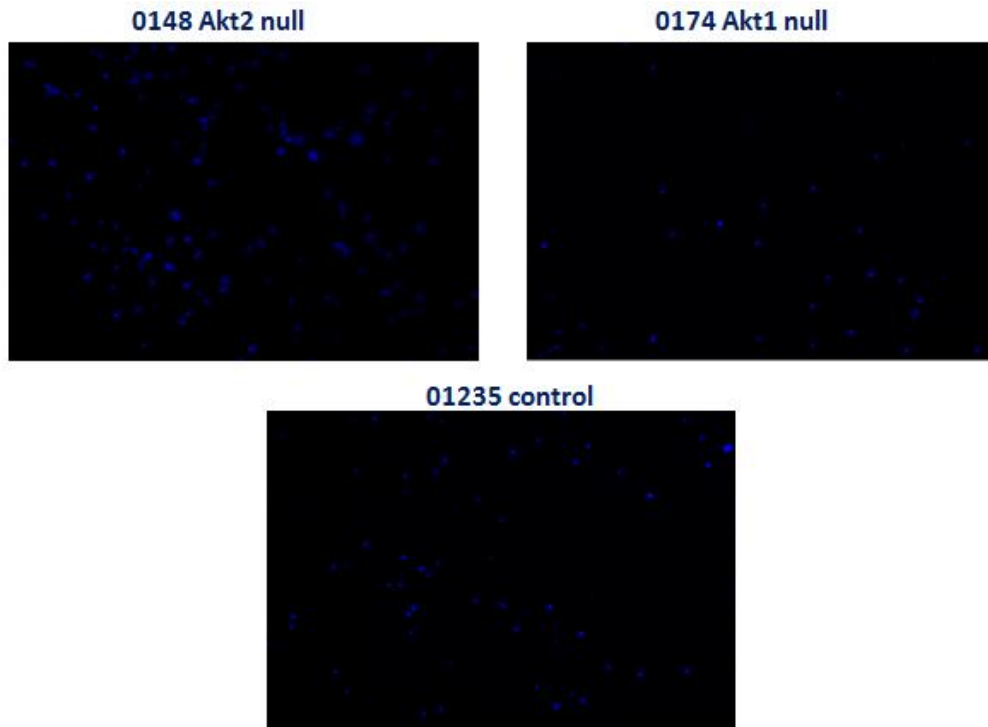


Figure 7 DAPI stained nuclei in representative fields of the three cell types

The representative fields of the DAPI stained nuclei indicate that in the cells that do not have Akt1, 0174 Akt1 null cells, have the least number of cells invaded to the lower side of the membrane when compared to the cells that retain Akt1 isoform. 0148 Akt2 null cells show more cells invaded than 01235 control cells.

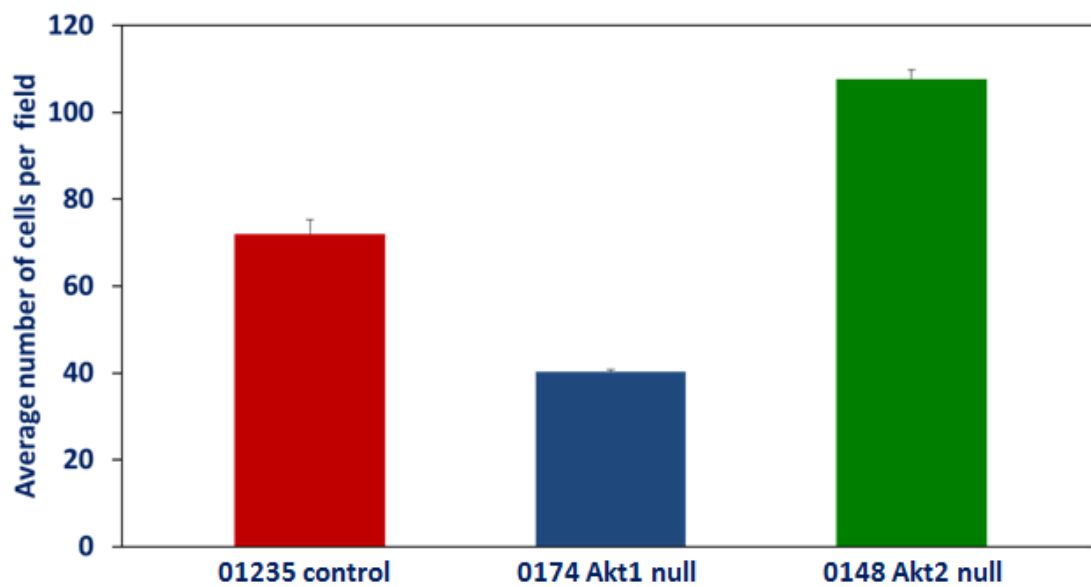


Figure 8 Quantitative comparison of the invaded cells between three cell types

Figure 6 shows the plot of average number of cells per field in each cell type. In 0148 Akt2 null cells, average count was 107 cells, 01235 controls showed an average count of 72 cells whereas 0174 Akt1 null cells had an average of 40 cells that invaded to the lower side of the membrane. This assay also gives an indication that Akt1 is essential for cell migration and invasion.

### **3.4 Induction of EMT**

A combination of TGF  $\beta$ 1 and EGF was used to induce EMT characteristics in the cells (Xu, Lao et al. 2012). At concentrations of 100 ng/ml of TGF  $\beta$ 1 and 1 ng/ml of EGF, it was observed that combination treatment with the two growth factors induced EMT in the cells 48 hours after treatment.

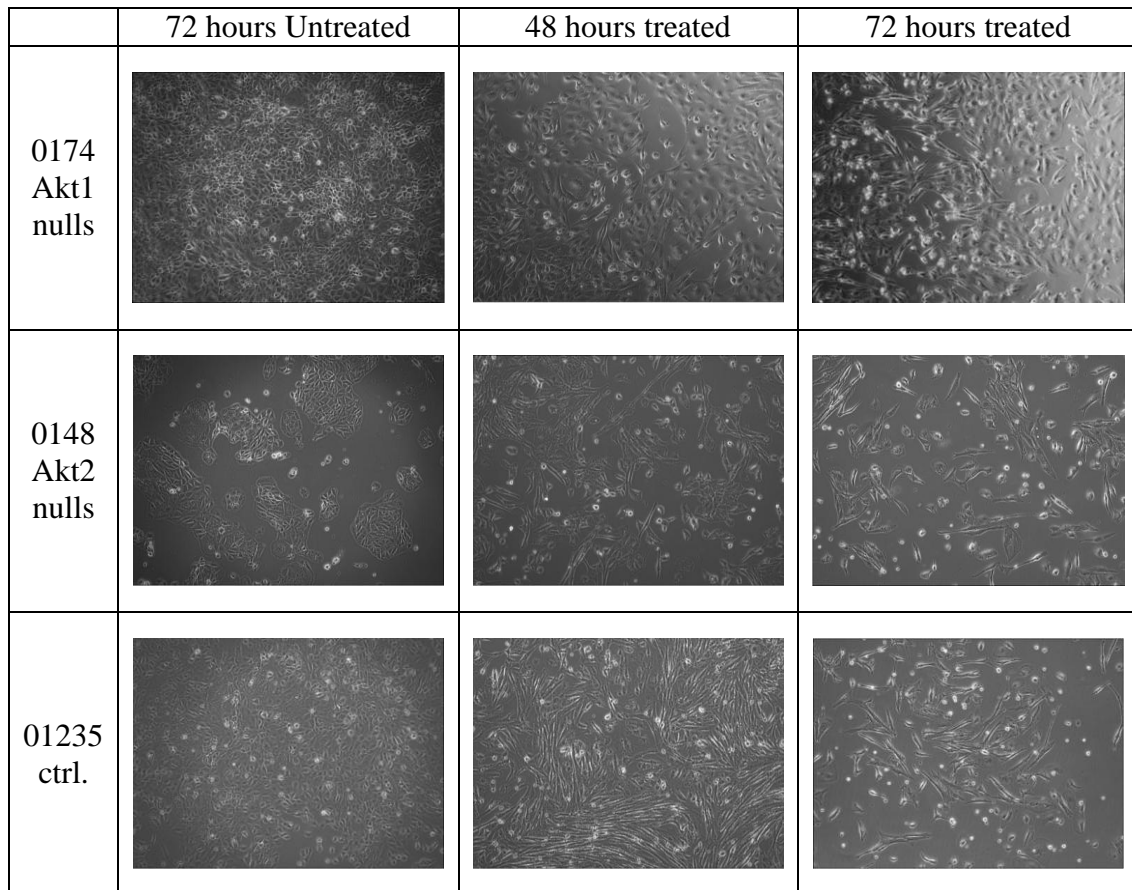


Figure 9 Change in morphology from epithelial to mesenchymal at 48 hours and 72 hours using TGF  $\beta$ 1 and EGF synergy. These images are representative of experiment performed in triplicates.

There is a difference in morphology from epithelial shape (as seen in 48 hours untreated column for all the three types) to mesenchymal spindle shaped cells (as seen in the 48 hours and 72 hours treatment columns).

Induction of EMT using 100 ng/ml TGF  $\beta$ 1 alone was also seen after 96 hours. This indicates that the positive influence between two growth factors TGF  $\beta$ 1 and EGF accelerated the process of EMT induction in the cells.

### **3.5 RT<sup>2</sup> Profiling using EMT array (PAMM-090 SABiosciences)**

Using EMT array analysis it was possible to test if there were any differences in the association of transcription factors and other players of EMT, with the two different Akt isoforms. The EMT array comprised of 84 genes implicated in the overall process of EMT. Three sets of experiments were prepared of cells with and without induction of EMT using TGF  $\beta$ 1 and EGF. RNA was collected from all the cells in the purest quality possible as defined by the  $A_{260}:A_{280}$  and  $A_{260}:A_{230}$  values.

Table 6 Concentration and Purity of Isolated RNA from samples with and without induction of EMT for RT<sup>2</sup> profiling

	Sample	Conc. ( $\mu\text{g}/\mu\text{l}$ )	$A_{260}:A_{280}$	$A_{260}:A_{230}$
Set 1	0174 Akt1 null not induced	1.110	2.02	1.80
	0148 Akt2 null not induced	0.805	1.97	1.36
	01235 controls not induced	1.187	2.03	1.81
	0174 Akt1 null EMT induced	0.851	2.03	1.64
	0148 Akt2 null EMT induced	0.773	2.04	1.61
	01235 control EMT induced	0.781	2.04	1.74
Set 2	0174 Akt1 null not induced	1.287	1.93	1.90
	0148 Akt2 null not induced	1.26	1.87	2.12
	01235 controls not induced	1.712	1.93	2.15
	0174 Akt1 null EMT induced	0.3408	1.87	1.88
	0148 Akt2 null EMT induced	1.424	1.93	2.13
	01235 control EMT induced	1.712	1.93	2.15
Set 3	0174 Akt1 null not induced	0.6979	1.96	2.05
	0148 Akt2 null not induced	0.4785	1.91	2.12
	01235 wild type not induced	0.519	1.90	2.10
	0174 Akt1 null EMT induced	1.774	2.0	2.21
	0148 Akt2 null EMT induced	0.8737	1.95	2.22
	01235 control EMT induced	1.067	1.98	2.20

After determining RNA concentration and purity, it was used for RT<sup>2</sup> profiling of EMT array. Table 7 shows the list of the genes that can be tested using this array.

Table 7 GENE Table listing the genes probed in RT<sup>2</sup> PCR Array Profiling

<b>Position</b>	<b>Symbol</b>	<b>Description</b>
A01	Ahnak	AHNAK nucleoprotein (desmoyokin)
A02	Akt1	Thymoma viral proto-oncogene 1
A03	Bmp1	Bone morphogenetic protein 1
A04	Bmp7	Bone morphogenetic protein 7
A05	Cald1	Caldesmon 1
A06	Camk2n1	Calcium/calmodulin-dependent protein kinase II inhibitor 1
A07	Cav2	Caveolin 2
A08	Cdh1	Cadherin 1
A09	Cdh2	Cadherin 2
A10	Col1a2	Collagen, type I, alpha 2
A11	Col3a1	Collagen, type III, alpha 1
A12	Col5a2	Collagen, type V, alpha 2
B01	Ctnnb1	Catenin (cadherin associated protein), beta 1
B02	Dsc2	Desmocollin 2
B03	Dsp	Desmoplakin
B04	Egfr	Epidermal growth factor receptor
B05	ErbB3	V-erb-b2 erythroblastic leukemia viral oncogene homolog 3 (avian)
B06	Esr1	Estrogen receptor 1 (alpha)
B07	F11r	F11 receptor
B08	Fgfbp1	Fibroblast growth factor binding protein 1
B09	<td>Fibronectin 1</td>	Fibronectin 1
B10	Foxc2	Forkhead box C2
B11	Fzd7	Frizzled homolog 7 (Drosophila)
B12	Gng11	Guanine nucleotide binding protein (G protein), gamma 11
C01	Gsc	Goosecoid homeobox
C02	Gsk3b	Glycogen synthase kinase 3 beta
C03	Igfbp4	Insulin-like growth factor binding protein 4
C04	Il1rn	Interleukin 1 receptor antagonist
C05	Ilk	Integrin linked kinase
C06	Itga5	Integrin alpha 5 (fibronectin receptor alpha)
C07	Itgav	Integrin alpha V
C08	Itgb1	Integrin beta 1 (fibronectin receptor beta)
C09	Jag1	Jagged 1
C10	Krt14	Keratin 14
C11	Krt19	Keratin 19
C12	Krt7	Keratin 7
D01	Mitf	Microphthalmia-associated transcription factor
D02	Mmp2	Matrix metalloproteinase 2
D03	Mmp3	Matrix metalloproteinase 3
D04	Mmp9	Matrix metalloproteinase 9
D05	Msn	Moesin
D06	Mst1r	Macrophage stimulating 1 receptor



<b>Position</b>	<b>Symbol</b>	<b>Description</b>
D07	Mtap1b	Microtubule-associated protein 1B
D08	Nodal	Nodal
D09	Notch1	Notch gene homolog 1 (Drosophila)
D10	Nudt13	Nudix (nucleoside diphosphate linked moiety X)-type motif 13
D11	Ocln	Occludin
D12	Pdgfrb	Platelet derived growth factor receptor, beta polypeptide
E01	Plek2	Pleckstrin 2
E02	Pppde2	PPPDE peptidase domain containing 2
E03	Ptk2	PTK2 protein tyrosine kinase 2
E04	Ptp4a1	Protein tyrosine phosphatase 4a1
E05	Rac1	RAS-related C3 botulinum substrate 1
E06	Rgs2	Regulator of G-protein signaling 2
E07	Serpine1	Serine (or cysteine) peptidase inhibitor, clade E, member 1
E08	Sip1	Survival of motor neuron protein interacting protein 1
E09	Smad2	MAD homolog 2 (Drosophila)
E10	Snai1	Snail homolog 1 (Drosophila)
E11	Snai2	Snail homolog 2 (Drosophila)
E12	Snai3	Snail homolog 3 (Drosophila)
F01	Sox10	SRY-box containing gene 10
F02	Sparc	Secreted acidic cysteine rich glycoprotein
F03	Spp1	Secreted phosphoprotein 1
F04	Stat3	Signal transducer and activator of transcription 3
F05	Steap1	Six transmembrane epithelial antigen of the prostate 1
F06	Tcf7l1	Transcription factor 7-like 1 (T-cell specific, HMG box)
F07	Tcf4	Transcription factor 4
F08	Tfpi2	Tissue factor pathway inhibitor 2
F09	Tgfb1	Transforming growth factor, beta 1
F10	Tgfb2	Transforming growth factor, beta 2
F11	Tgfb3	Transforming growth factor, beta 3
F12	Timp1	Tissue inhibitor of metalloproteinase 1
G01	Tmeff1	Transmembrane protein with EGF-like and two follistatin-like domains 1
G02	Tmem132a	Transmembrane protein 132A
G03	Tspan13	Tetraspanin 13
G04	Twist1	Twist homolog 1 (Drosophila)
G05	Vcan	Versican
G06	Vim	Vimentin
G07	Vps13a	Vacuolar protein sorting 13A (yeast)
G08	Wnt11	Wingless-related MMTV integration site 11
G09	Wnt5a	Wingless-related MMTV integration site 5A
G10	Wnt5b	Wingless-related MMTV integration site 5B
G11	Zeb1	Zinc finger E-box binding homeobox 1
G12	Zeb2	Zinc finger E-box binding homeobox 2
H01	Gusb	Glucuronidase, beta
H02	Hprt	Hypoxanthine guanine phosphoribosyl transferase

<b>Position</b>	<b>Symbol</b>	<b>Description</b>
H03	Hsp90ab1	Heat shock protein 90 alpha (cytosolic), class B member 1
H04	Gapdh	Glyceraldehyde-3-phosphate dehydrogenase
H05	Actb	Actin, beta
H06	MGDC	Mouse Genomic DNA Contamination
H07	RTC	Reverse Transcription Control
H08	RTC	Reverse Transcription Control
H09	RTC	Reverse Transcription Control
H10	PPC	Positive PCR Control
H11	PPC	Positive PCR Control
H12	PPC	Positive PCR Control

On complete analysis of three sets of the same sample using the online analysis programs provided by SABiosciences (<http://pcrdataanalysis.sabiosciences.com/pcr/arrayanalysis.php>) it was observed that there is a difference in regulation of certain genes in an isoform specific manner, as discussed below.

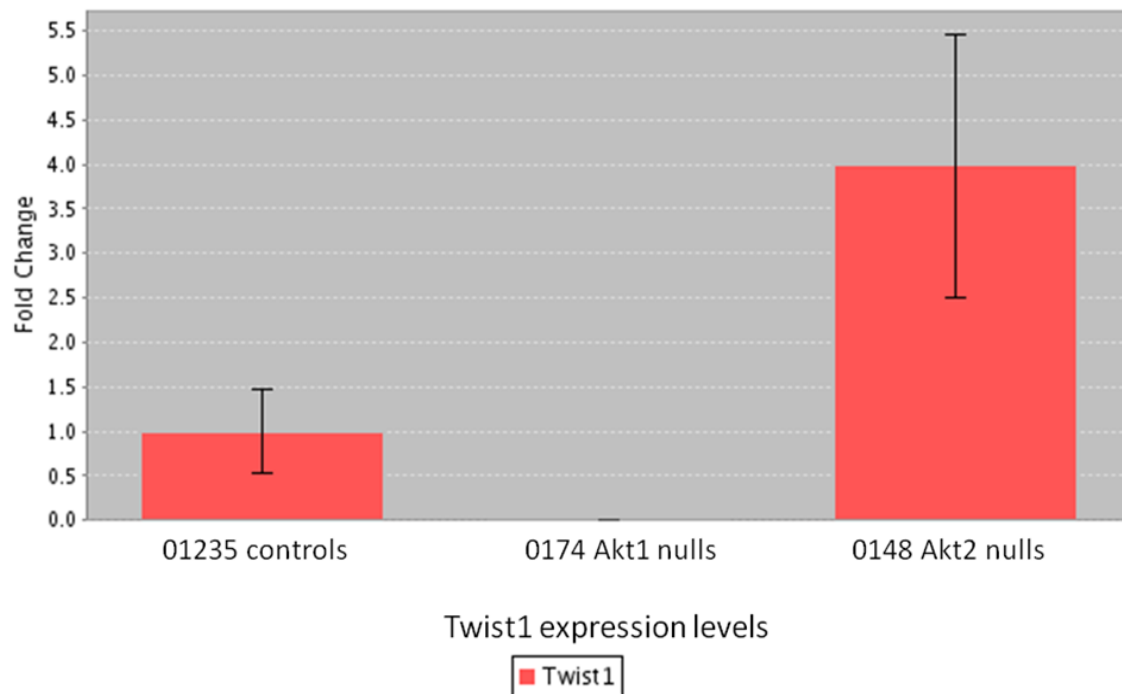


Figure 10 Comparison of fold change regulation of Twist1 expression levels in 01235 tumor cells with retention of Akt1 and Akt2 (controls), 0174 Akt1 nulls and 0148 Akt2 nulls

Twist1, a basic helix-loop-helix transcription factor with a major role in EMT, was not expressed in the cells missing Akt1 expression. (Ct values were obtained as raw data from the cyclor and were processed to calculate  $\Delta Ct$  and  $\Delta\Delta Ct$  values in order to calculate gene expression. Ct value is defined as the number of cycles to cross the threshold value (exceeds background level) required for the fluorescent signal. The expression of Twist1 was retained in the cells having Akt1, in both control tumor cells and Akt2 null cells as shown in Figure 8. A similar pattern was found in the samples collected from the cells treated for EMT induction. Even though EMT was induced, which was confirmed by the change in cellular morphology as shown in Figure 7, expression of Snai2 (Slug) was reduced and Twist1 was missing in Akt1 null cells.

Snai2 (Slug) – Snai family player implicated in EMT, showed a similar pattern as Twist1. Loss of Akt1 reduced expression of Slug whereas Akt1 presence showed expression of Slug as demonstrated in Figure 9.

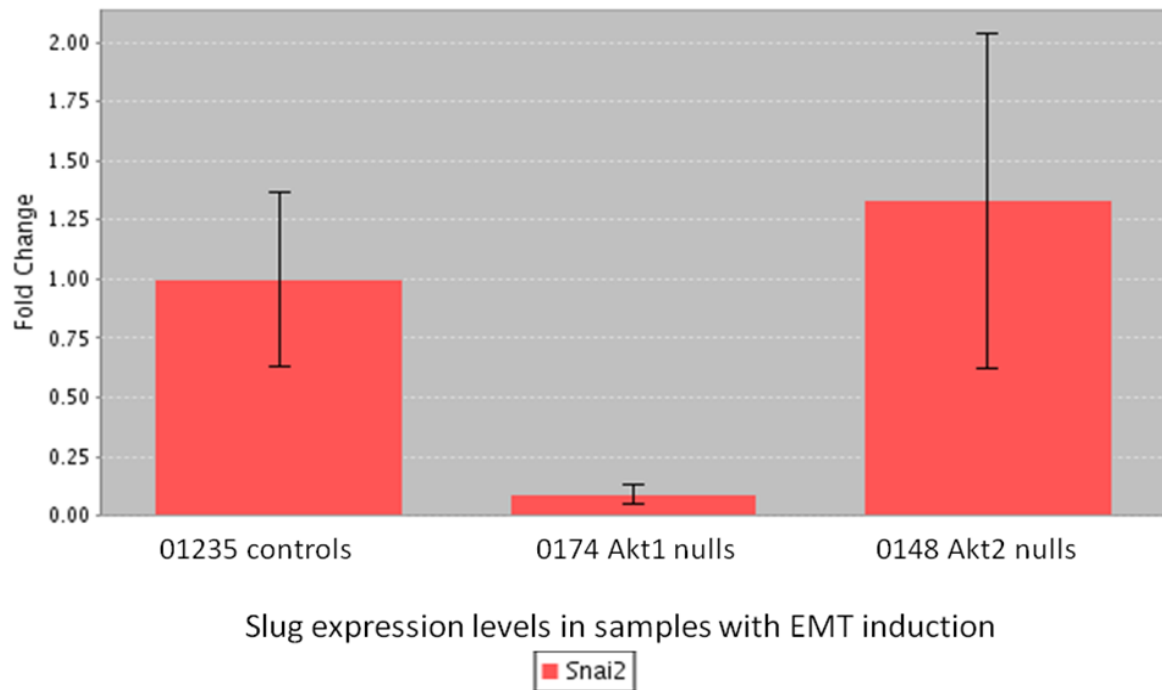


Figure 11 Comparison of fold change regulation of Snai2 (Slug) expression levels in 01235 tumor cells with retention of Akt1 and Akt2 (controls), 0174 Akt1nulls and 0148 Akt2 nulls

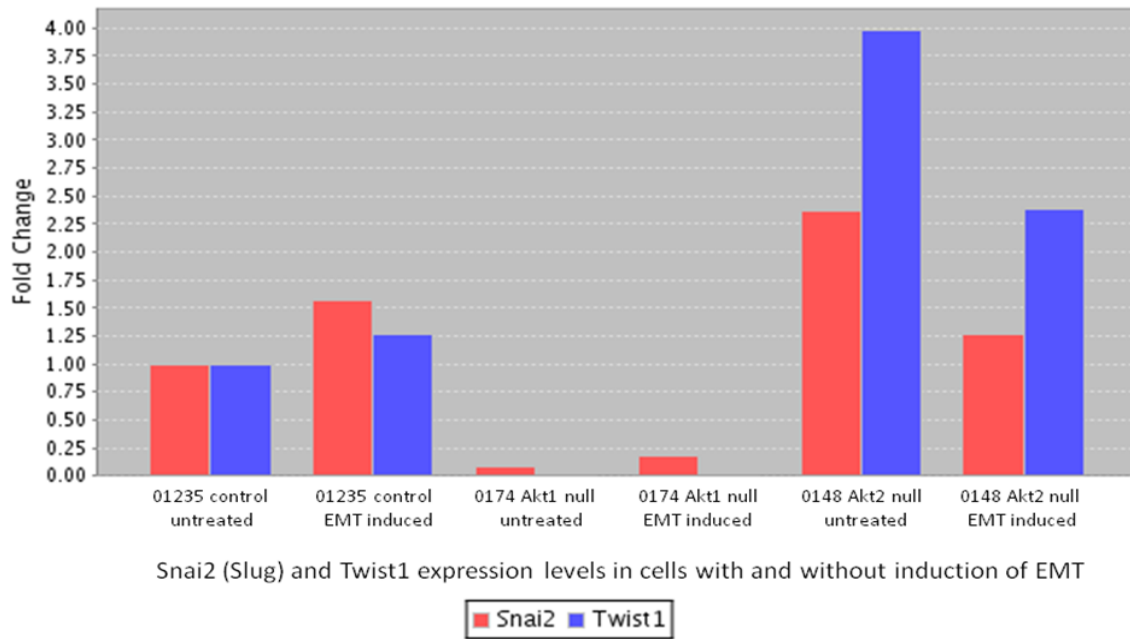


Figure 12 Comparison of fold change regulation of Snai2 (Slug) and Twist1 expression levels in 01235 tumor cells with retention of Akt1 and Akt2 (controls), 0174 Akt1nulls and 0148 Akt2 nulls with and without induction of EMT

These experiments were conducted in triplicates in order to be able to establish statistical significance in the form of P-values.

Table 8 P-values of Snai2 and Twist1 calculated from the samples in triplicates of the groups with and without EMT induced.

	Snai2	Twist1
0174 Akt1 null cells	0.040509	0.00792
0148 Akt2 null cells	0.046475	0.013656

Analysis of the Real time PCR data also indicated certain candidates, which were over expressed or de-regulated in the two different isoforms.

Table 9 Fold regulation values determining over or under expression of genes in 0174 Akt1 null cells when compared to 01235 controls.

<b>Gene Symbol</b>	<b>Fold Regulation Over expressed</b>	<b>Gene Symbol</b>	<b>Fold Regulation Under expressed</b>
Bmp7	37.5942	Col3a1	-4.6443
Col1a2	36.8143	Col5a2	-16.5536
Dsc2	26.7498	Esr1	-19.8141
Fgfbp1	5.4569	Fn1	-5.5858
Il1rn	19.8512	Gng11	-12.3894
Krt19	119.5645	Mmp3	-8.3825
Ocln	23.842	Serpine1	-4.7551
Snai3	7.5474	Snai2	-11.2836
Sox10	4.1922	Tspan13	-88.8907
Spp1	5.9393	Twist1	-4734.3843
Vcan	4.2		

Table 10 Fold regulation values determining over or under expression of genes in 0148 Akt2 null cells when compared to 01235 controls.

<b>Gene Symbol</b>	<b>Fold Regulation Over expressed</b>	<b>Gene Symbol</b>	<b>Fold Regulation Under expressed</b>
Bmp7	61.2847	Cald1	-4.0133
Fgfbp1	15.7639	Cdh1	-7.8847
Igfbp4	8.6613	Il1rn	-8.7068
Krt19	25.6732	Mtap1b	-5.9455
Pdgfrb	5.1161	Serpine1	-8.4769
Rgs2	13.1008	Spp1	-80.9743
Tgfb2	16.0138	Vcan	-60.0882
Tgfb3	5.4213		
Tmem132a	4.4083		
Tspan13	75.715		

Table 11 Fold regulation values determining over or under expression of genes in 0174 Akt1 null cells when compared to 0148 Akt2 null.

<b>Gene Symbol</b>	<b>Fold Regulation Over expressed</b>	<b>Gene Symbol</b>	<b>Fold Regulation Under expressed</b>
Col1a2	75.3493	Bmp1	-4.7141
Dsc2	98.8236	Col3a1	-8.5963
Il1rn	172.8414	Col5a2	-4.5213
Jag1	4.804	Egfr	-4.0675
Krt19	4.6572	Esr1	-71.1346
Mmp2	7.5597	Fn1	-7.0982
Ocln	37.071	Foxc2	-4.0881
Snai3	11.2095	Gsk3b	-4.1318
Sox10	4.1506	Igfbp4	-6.1823
Spp1	480.9273	Mmp3	-11.6224
Vcan	252.368	Ptp4a1	-5.862
		Rgs2	-6.4562
		Snai2	-26.8049
		Tcf4	-4.1073
		Tgfb2	-8.6617
		Tspan13	-6730.3577
		Twist1	-18850.5551
		Wnt5a	-4.7863



### 3.6 Validation at Protein levels

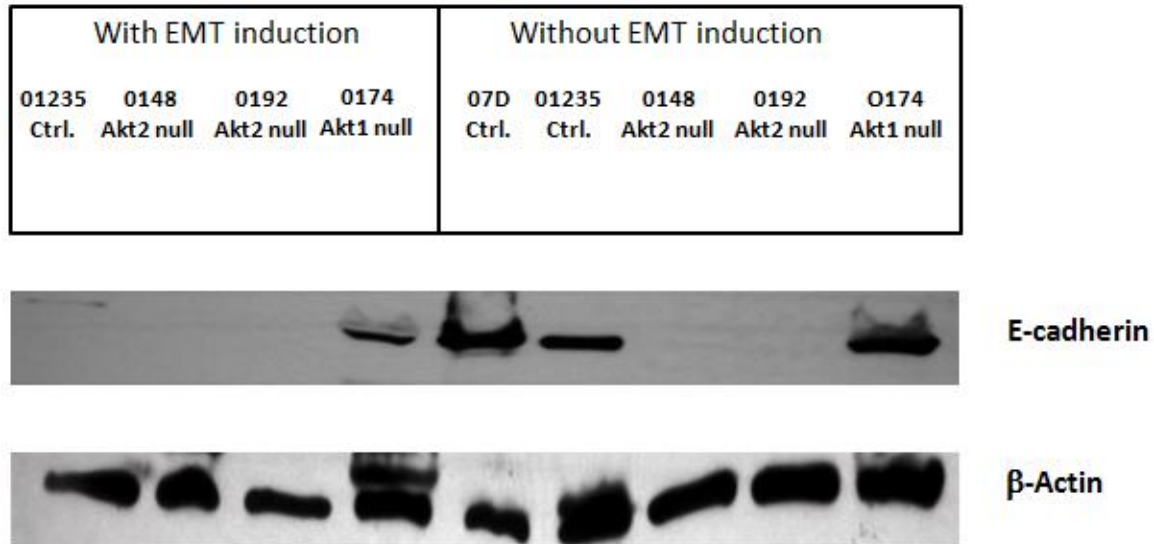


Figure 13 Validation of real time findings using protein band determination. E-cadherin and  $\beta$ -actin antibodies (Cell Signaling) were used and samples with and without induction of EMT were analyzed.

The effect of reduced or no expression at RNA levels was seen on protein levels. E-cadherin, whose expression is reduced by Twist1, was probed on the protein extracted from samples with and without EMT induction. It is observed that the 0174 Akt1 null tumor cells missing Akt1 and Twist1 show bands for E-cadherin. The 0148 Akt2 null tumor cells with Akt1 expression and thus Twist1 expression do not show E-cadherin bands at protein levels. The appearance of E-cadherin bands in the cells with both Akt1 and Akt2 expression might be due to the compensatory mechanisms working between the two isoforms.

## CHAPTER 4. DISCUSSION

The Akt family of kinases is one of the most versatile players in cell biology affecting various cell processes namely proliferation, metabolism, survival, tumor development and EMT (Xue, Restuccia et al. 2012). This family of three important kinases Akt1, 2 and 3 has been widely studied for their implications in various cancers. With advancing literature updates it has been observed that Akt isoforms might have a tissue specific function in a matured tumor phenotype. There have been conflicting studies debating the role and mechanism of Akt1 isoform in inhibition of cell motility and invasion in human breast cancer tissue. One study states that it is independent of ERK pathway, whereas another states proteosomal degradation of NFAT by Akt1 (Liu, Radisky et al. 2006). There has been evidence of Akt2 being transcriptionally up-regulated by Twist1 in breast cancer tissue (Cheng, Chan et al. 2007). On the contrary, in lung cancer Akt1 is the predominant regulator of both proliferation and migration when compared to Akt2. These conflicting roles of Akt isoforms in different tissues affirm the need to delineate their roles in ovarian cancer. Using transgenic mice, in this study one type of tumor cells were derived from mice with genetic inactivation of Akt1 (0174 Akt1 knockout), other types with genetic inactivation of Akt2 (0148 Akt2 knockout) and a third type with retention of both Akt1 and Akt2 (01235 control).

While observing the cell migratory patterns using wound healing assays in the three different types of cells stated above, it was observed that Akt1 retention enhanced the migration of cells. Akt1 knockout cells had reduced migration rates. This result suggests a tissue specific reversal of roles of Akt1 when compared to human breast cancer tissue where Akt1 is said to

have anti-migratory role. Similar patterns were established with every repeat of the wound healing assay where the 0174 Akt1 knockout cells took much longer time to fill up the wound when compared to the cells with retention of Akt1 – 0148 Akt2 nulls and 01235 controls. Cell migration was tested using a different assay where the invasiveness of the cells was gauged using the BD BioCoat Matrigel Invasion chambers. Results obtained using this assay were similar to those of the wound healing assay. The wells containing Akt1 knockout cells demonstrated less invasive potential.

The ability of tumor cells to migrate contributes to the metastasis of the tumor cells and is governed by a phenomenon called as epithelial-mesenchymal transition (EMT). EMT, a normal and necessary mechanism during embryonic development and embryogenesis, is undesirable and causes metastasis in cancers with advanced tumor stages. The signaling proteins involved in EMT remain more or less the same during both embryogenesis and metastasis. In order to obtain a better understanding about the role of Akt1 pertaining to cell migration, it was decided to look for unique differences in transcription factors involved in EMT. Real time PCR array (SAbiosciences, Qiagen) analysis involving 84 genes highly implicated in EMT was performed. There was a striking observation noted wherein the 0174 Akt1 knockout cells did not exhibit expression of Twist1, whereas cells with retention of Akt1 (0148 Akt2 knockouts and 01235 controls) exhibited expression of Twist1 to a significant extent. Twist1 is a basic helix-loop-helix transcription factor, which plays a very important role in EMT by suppressing the expression of E-cadherin. E-cadherin holds the cells in epithelial phenotype and down regulation of E-cadherin is found in mesenchymal phenotype or the cells that have highly metastasized. By knocking out Akt1, Twist1 expression levels were not detectable and this might be one of the main reasons

why the Akt1 knockout cells took longer time to migrate and fill in the wound assay and also show less invasiveness. Similar patterns were found in Snai2 (Slug), another important regulator of EMT. There have been reports of the association of Akt2 with Twist1 in human breast cancer cells and further rationalizing of the role of Akt2 as an enhancer of cell migration in human breast cancer cells. With the RT profile analysis presented here there is an indication of a novel link, which could be used to establish that in murine ovarian tumor cells, Akt1 is associated with Twist1, thus rationalizing role of Akt1 as an enhancer of cell migration and invasion.

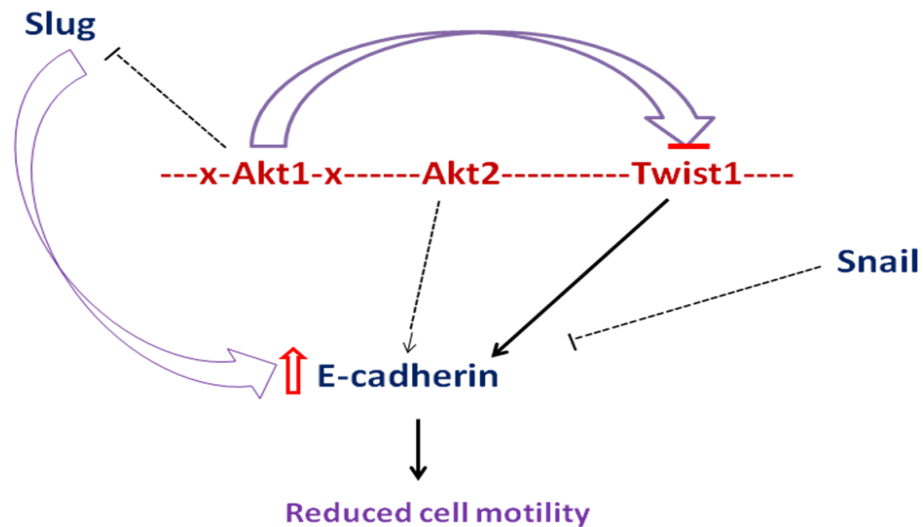


Figure 14 A Schematic, indicating the series of events that may explain the observations in the cell model. Genetic inactivation of Akt1 leads to reduced expression of Twist1 and Slug, which in turn could not completely inhibit expression of E-cadherin. The reduced E-cadherin levels may be due to Snail whose expression seems to be governed independent of the Akt isoform knockouts. Overall this phenomenon causes reduced motility in the Akt1 null cells. It could also be possible that Akt2 is responsible for expression of E-cadherin.

The validity of this link was further tested by inducing EMT in the cells using a synergy between TGF  $\beta$ 1 and EGF. There was a drastic change in morphology of the cells from epithelial to mesenchymal phenotype observed after 48 hours. The RT profile analysis showed a similar pattern of Twist1 missing in the cells without Akt1 and over expression of Twist1 in cells retaining Akt1.

EMT in ovarian carcinoma has a reputation of being an exception to the norm. Although certain EMT markers in ovarian cancer show similar pattern of over-expression during EMT as in other types of cancer, there are certain basic players like E-cadherin and N-cadherin whose regulation patterns are not consistent with the data from other types of cancer during high metastasis. RT profiles suggest similar unconventionalities of the same markers in ovarian tumor cells used for my project. Typically E-cadherin should be repressed during induction of EMT. The profiles indicate change in RNA expression of E-cadherin but this finding could be more closely related to presence of Twist1 than to induction of EMT. The presence of Twist1 in cells with Akt1 exhibited low expression levels of E-cadherin as compared to cells missing Akt1 and Twist1 where E-cadherin is expressed in normal levels.

There have been recent studies that suggest a cross talk between the PI3 kinase/Akt and TGF  $\beta$  signaling axes. The real time data indicate that the cells with loss of Akt1 exhibit reduced expression of TGF  $\beta$ 2. The cells retaining Akt1 and loss of Akt2 exhibit increased TGF  $\beta$ 2 and TGF  $\beta$ 3 expression levels. This might indicate isoform specific channeling of the cross-talk between the two signaling pathways.

The real time data is consistent to the speculation posed regarding the noncanonical nature of ovarian EMT. There is definitive link between Akt and EMT, where different isoforms

regulate protein effectors through specific associations. Since there are numerous players that might crosstalk to contribute to EMT, off-target regulation of one of the players does not block the process to a great significance aside from delaying the process. In spite of this robustness of EMT, clarifying the molecular mechanisms will increase the likelihood of improving therapeutic targeting.

Validation at protein levels was used to show a consistent pattern affecting Twist1 loss and appearance of bands of E-cadherin. 0174 Akt1 knockouts, which lack Twist1 expression at RNA levels, showed strong bands corresponding to E-cadherin protein after western blot analysis. The 0148 Akt2 knockouts retaining Akt1 showed no bands for E-cadherin. Protein extracted from the cells with EMT induction also showed similar pattern. E-cadherin protein expression was diminished in the induced samples, which is consistent with induction of EMT. Thus, it is postulated that EMT induction should lead to complete loss of E-cadherin, which happens in cells retaining Akt1, but cells with the loss of Akt1 and subsequent loss of Twist1 do not show complete inhibition of E-cadherin reassuring the association of Akt1 and Twist1 at functional levels.

This novel association between Akt1 and Twist1 in ovarian tumor cells needs to be further analyzed to understand the mechanistic link between the two. This could be achieved by silencing either of the two and in turn understanding the effect of one on the other. Although typically an exception to the norm, the data presented here suggest that EMT in ovarian cancer can be elucidated by understanding such novel links between the various hallmark cell signaling proteins like Akt, TGF  $\beta$  and transcription factors like Snail, Slug, Twist, Zeb family and others.

## REFERENCES

- Agarwal, R. and S. B. Kaye (2003). "Ovarian cancer: strategies for overcoming resistance to chemotherapy." Nat Rev Cancer **3**(7): 502-516.
- Ahmed, N., E. W. Thompson, et al. (2007). "Epithelial-mesenchymal interconversions in normal ovarian surface epithelium and ovarian carcinomas: an exception to the norm." J Cell Physiol **213**(3): 581-588.
- Alipio, Z. A., N. Jones, et al. (2011). "Epithelial to mesenchymal transition (EMT) induced by bleomycin or TFG(b1)/EGF in murine induced pluripotent stem cell-derived alveolar Type II-like cells." Differentiation **82**(2): 89-98.
- Altomare, D. A. and J. R. Testa (2005). "Perturbations of the AKT signaling pathway in human cancer." Oncogene **24**(50): 7455-7464.
- Bellacosa, A., D. de Feo, et al. (1995). "Molecular alterations of the AKT2 oncogene in ovarian and breast carcinomas." Int J Cancer **64**(4): 280-285.
- Bellacosa, A., J. R. Testa, et al. (1991). "A retroviral oncogene, akt, encoding a serine-threonine kinase containing an SH2-like region." Science **254**(5029): 274-277.
- Cannistra, S. A. (2004). "Cancer of the ovary." N Engl J Med **351**(24): 2519-2529.
- Carpten, J. D., A. L. Faber, et al. (2007). "A transforming mutation in the pleckstrin homology domain of AKT1 in cancer." Nature **448**(7152): 439-444.

- Cheng, G. Z., J. Chan, et al. (2007). "Twist transcriptionally up-regulates AKT2 in breast cancer cells leading to increased migration, invasion, and resistance to paclitaxel." Cancer Res **67**(5): 1979-1987.
- Cheng, J. Q., B. Ruggeri, et al. (1996). "Amplification of AKT2 in human pancreatic cells and inhibition of AKT2 expression and tumorigenicity by antisense RNA." Proc Natl Acad Sci U S A **93**(8): 3636-3641.
- Cho, K. R. and M. Shih Ie (2009). "Ovarian cancer." Annu Rev Pathol **4**: 287-313.
- Christiansen, J. J. and A. K. Rajasekaran (2006). "Reassessing epithelial to mesenchymal transition as a prerequisite for carcinoma invasion and metastasis." Cancer Res **66**(17): 8319-8326.
- Connolly, D. C., R. Bao, et al. (2003). "Female mice chimeric for expression of the simian virus 40 TAg under control of the MISIR promoter develop epithelial ovarian cancer." Cancer Res **63**(6): 1389-1397.
- Davidson, B. (2001). "Ovarian carcinoma and serous effusions. Changing views regarding tumor progression and review of current literature." Anal Cell Pathol **23**(3-4): 107-128.
- Davidson, B., C. G. Trope, et al. (2012). "Epithelial-mesenchymal transition in ovarian carcinoma." Front Oncol **2**: 33.
- Hennessy, B. T., R. L. Coleman, et al. (2009). "Ovarian cancer." Lancet **374**(9698): 1371-1382.
- Irie, H. Y., R. V. Pearline, et al. (2005). "Distinct roles of Akt1 and Akt2 in regulating cell migration and epithelial-mesenchymal transition." J Cell Biol **171**(6): 1023-1034.
- Jemal, A., R. Siegel, et al. (2010). "Cancer statistics, 2010." CA Cancer J Clin **60**(5): 277-300.



- Kalluri, R. and R. A. Weinberg (2009). "The basics of epithelial-mesenchymal transition." J Clin Invest **119**(6): 1420-1428.
- Landen, C. N., Jr., M. J. Birrer, et al. (2008). "Early events in the pathogenesis of epithelial ovarian cancer." J Clin Oncol **26**(6): 995-1005.
- Lee, M. W., D. S. Kim, et al. (2011). "Roles of AKT1 and AKT2 in non-small cell lung cancer cell survival, growth, and migration." Cancer Sci.
- Liu, H., D. C. Radisky, et al. (2006). "Mechanism of Akt1 inhibition of breast cancer cell invasion reveals a protumorigenic role for TSC2." Proc Natl Acad Sci U S A **103**(11): 4134-4139.
- Maestro, R., A. P. Dei Tos, et al. (1999). "Twist is a potential oncogene that inhibits apoptosis." Genes Dev **13**(17): 2207-2217.
- Mayo, L. D. and D. B. Donner (2001). "A phosphatidylinositol 3-kinase/Akt pathway promotes translocation of Mdm2 from the cytoplasm to the nucleus." Proc Natl Acad Sci U S A **98**(20): 11598-11603.
- Nicholson, K. M. and N. G. Anderson (2002). "The protein kinase B/Akt signalling pathway in human malignancy." Cell Signal **14**(5): 381-395.
- Patel, I. S., P. Madan, et al. (2003). "Cadherin switching in ovarian cancer progression." Int J Cancer **106**(2): 172-177.
- Shan, W. and J. Liu (2009). "Epithelial ovarian cancer: focus on genetics and animal models." Cell Cycle **8**(5): 731-735.
- Singer, G., R. Oldt, 3rd, et al. (2003). "Mutations in BRAF and KRAS characterize the development of low-grade ovarian serous carcinoma." J Natl Cancer Inst **95**(6): 484-486.

- Sundfeldt, K., K. Ivarsson, et al. (2001). "Higher levels of soluble E-cadherin in cyst fluid from malignant ovarian tumours than in benign cysts." Anticancer Res **21**(1A): 65-70.
- Testa, J. R. and A. Bellacosa (2001). "AKT plays a central role in tumorigenesis." Proc Natl Acad Sci U S A **98**(20): 10983-10985.
- Thiery, J. P., H. Acloque, et al. (2009). "Epithelial-mesenchymal transitions in development and disease." Cell **139**(5): 871-890.
- Thompson, E. W., D. F. Newgreen, et al. (2005). "Carcinoma invasion and metastasis: a role for epithelial-mesenchymal transition?" Cancer Res **65**(14): 5991-5995; discussion 5995.
- Vivanco, I. and C. L. Sawyers (2002). "The phosphatidylinositol 3-Kinase AKT pathway in human cancer." Nat Rev Cancer **2**(7): 489-501.
- Xu, N., Y. Lao, et al. (2012). "Akt: a double-edged sword in cell proliferation and genome stability." J Oncol **2012**: 951724.
- Xue, G., D. F. Restuccia, et al. (2012). "Akt/PKB-mediated phosphorylation of Twist1 promotes tumor metastasis via mediating cross-talk between PI3K/Akt and TGF-beta signaling axes." Cancer Discov **2**(3): 248-259.
- Yang, J. and R. A. Weinberg (2008). "Epithelial-mesenchymal transition: at the crossroads of development and tumor metastasis." Dev Cell **14**(6): 818-829.
- Yap, T. A., M. D. Garrett, et al. (2008). "Targeting the PI3K-AKT-mTOR pathway: progress, pitfalls, and promises." Curr Opin Pharmacol **8**(4): 393-412.
- Yoeli-Lerner, M., G. K. Yiu, et al. (2005). "Akt blocks breast cancer cell motility and invasion through the transcription factor NFAT." Mol Cell **20**(4): 539-550.

Zeisberg, M. and E. G. Neilson (2009). "Biomarkers for epithelial-mesenchymal transitions." J Clin Invest **119**(6): 1429-1437.